Recent advances in aptasensors based on graphene and graphene-like nanomaterials

Ping, Jianfeng; Zhou, Yubin; Wu, Yuanyuan; Papper, Vladislav; Boujday, Souhir; Marks, Robert S.; Steele, Terry W. J.

2014

Ping, J., Zhou, Y., Wu, Y., Papper, V., Boujday, S., Marks, R. S., et al. (2015). Recent advances in aptasensors based on graphene and graphene-like nanomaterials. Biosensors and Bioelectronics, 64, 373-385.

https://hdl.handle.net/10356/80570

https://doi.org/10.1016/j.bios.2014.08.090

Recent advances in aptasensors based on graphene and graphene-like nanomaterials

Jianfeng Ping[a,†], Yubin Zhou[a,†], Yuanyuan Wu[a], Vladislav Papper[a], Souhir Boujday[b,c], Robert S. Marks[d], Terry W. J. Steele[a,*]

[a] *School of Materials Science & Engineering, College of Engineering, Nanyang Technological University, 50 Nanyang Avenue, Singapore 639798, Singapore*

[b] *Sorbonne Universités, UPMC, Univ Paris 6, UMR CNRS 7197, Laboratoire de Réactivité de Surface, F75005 Paris, France*

[c] *CNRS, UMR 7197, Laboratoire de Réactivité de Surface, F75005 Paris, France*

[d] *Department of Biotechnology Engineering, Faculty of Engineering Sciences, Ben Gurion University of the Negev, P.O. Box 653, Beer Sheva 84105, Israel*

[*] *Corresponding Author. Tel.:65-65927594; fax: 65-67909081.*

E-mail address: wjsteele@ntu.edu.sg

[†] *These authors contributed equally to this work.*

ABSTRACT

Graphene and graphene-like two-dimensional nanomaterials have aroused tremendous research interest in recent years due to their unique electronic, optical, and mechanical properties associated with their planar structure. Aptamers have exhibited many advantages as molecular recognition elements for sensing devices compared to traditional antibodies. The marriage of two-dimensional nanomaterials and aptamers has emerged many ingenious aptasensing strategies for applications in the fields of clinical diagnosis and food safety. This review highlights current advances in the development and application of two-dimensional nanomaterials-based aptasensors with the focus on two main signal-transducing mechanisms, i.e. electrochemical and optical. A special attention is paid to graphene, a one-atom thick layer of graphite with exceptional properties, representing a fastgrowing field of research. In view of the unique properties of two-dimensional nanostructures and their inherent advantages of synthetic aptamers, we expect that high-performance two-dimensional nanomaterials-based aptasensing devices will find extensive applications in environmental monitoring, biomedical diagnostics, and food safety.

Keywords:

Aptasensor

Biosensor

Graphene

Aptamer

Two-dimensional nanomaterial

Content

1. Introduction

Nanomaterials have been employed to construct sensing devices in view of their unique electronic, optical, mechanical, and thermal properties. With the past decades, a new wave of research on the biosensors has focused on the combination of nanomaterials with molecular recognition elements (Wang et al., 2010a; Yang et al., 2010). Among the plethora of nanomaterials, two-dimensional nanomaterials have emerged as promising nanoplatforms. These next generation nanostructures have inherent superior light absorbance and rapid electron transfer rate (Georgakilas et al., 2012; Koski and Cui, 2013). Specifically, the unique planar structure and sizable specific surface areas would enlarge the loading efficiency and surface concentration of biomolecule (Chen et al., 2012b; Mao et al., 2013). Therefore, the integration of two-dimensional nanomaterials with aptamers could bring about many attractive opportunities for the development of novel aptasensors with enhanced performance. Here, we review the current research literature on two-dimensional nanomaterials-based aptasensors. Different aptasensing strategies along with different signal-transducing mechanisms and different combination modes of aptamers with two-dimensional nanomaterials are discussed. Our aim is to give the reader a complete concept about the recent advances of two-dimensional nanomaterials-based aptasensors and expect more two-dimensional nanostructures and more synthetic aptamers be enrolled into this research field that create really workable biosensing devices serving for human world.

Aptamers, generated from “systematic evolution of ligands by exponential enrichment” (SELEX) technique, are short single-stranded oligonucleotides (DNA or RNA) that bind to specific targets similarly as antibodies, drawing extensive attention from both the theoretical and experimental scientific communities since their discovery in 1990 (Ellington and Szostak, 1990; Robertson and Joyce, 1990; Tuerk and Gold, 1990). Aptamers act as molecular recognition elements whose purpose is to recognize and bind to their targets with excellent affinity (the dissociation constants

K_d ranging from micromolar to picomolar levels) by folding themselves into distinct secondary or tertiary structures (Lubin and Plaxco, 2010; Wang et al., 2012f). The targets range from small organic molecules, metal ions, proteins, biological cells, to tissues (Amaya-Gonzalez et al., 2013). In addition, aptamers also exhibit other unique features over antibodies, such as *in vitro* selection, chemical stability, low immunogenicity, automated synthesis and numerous choices of nucleotide or phosphate functional groups (Du et al., 2013b). These exceptional properties make aptamers capable of serving as favorable molecular recognition elements in the design of high-performance biosensing devices (i.e., aptasensors) (Li et al., 2010; Vinkenborg et al., 2011) and reviews dealing with their biosensing strategies were published recently (Famulok and Mayer, 2011; Hong et al., 2012; Lim et al., 2010; Liu et al., 2009; Meir et al., 2007; Zhou et al., 2010).

Since the discovery of graphene, the field of two-dimensional nanomaterials has grown extensively over the past decade. So far, the family of two-dimensional nanomaterials has extended from graphene and its derivatives (like graphene oxide, fluorographene, graphane, etc.) to transition metal chalcogenides (such as MoS_2, WS_2, $MoSe_2$, WSe_2, etc.), metal oxides (like MoO_3, WO_3, MnO_2, $Ni(OH)_2$, etc.), and other layered compounds with the common feature that the bulk three-dimensional crystals of these layered materials are stacked structures held together through their van der Waals forces among adjacent layers (Leonard and Talin, 2011; Xu et al., 2013a). A library of current two-dimensional crystals was made by Geim and Grigorieva (2013). By consecutive thinning of the bulk layered structures to monolayer or few-layer dimensions (i.e. two-dimensional), many intriguing properties are observed, such as topological insulator effect, superconductivity, and thermoelectricity (Govindaraju and Avinash, 2012; Koski and Cui, 2013).

Among these reported two-dimensional crystals, graphene deserves special recognition in view of its distinctive structure and exceptional physical properties (Novoselov et al., 2004). Graphene is a sheet of sp^2 bonded carbon atoms that are

arranged into a rigid honeycomb lattice, exhibiting the highest mechanical strength among the known materials, extraordinary electron transfer capabilities, excellent electrical conductivity, ultra-large specific surface area, unprecedented pliability and impermeability, and favorable biocompatibility (Balandin, 2011; Craciun et al., 2011). Additionally, the methods of graphene synthesis have undergone substantial development in the past decade to meet various application requirements. Some examples of synthetic methods include mechanical exfoliation, chemical vapor method, chemical and electrochemical reduction methods to obtain either pristine graphene, single-layer graphene with designed plane size, or graphene composites directly from graphite, respectively (Park and Ruoff, 2009; Zhang et al., 2012a). All these promote the application prospects of graphene in electronic devices, energy generation and storage, sensors, DNA sequencing, and hybrid materials (Mao et al., 2013; Wu et al., 2007).

Regarding the aptasensor development, graphene looks like to have the necessary requirements to implement next generation, and high-performance aptasensors (Kuila et al., 2011). More importantly, graphene has a natural gift to noncovalent adsorption of the unfolded aptamer (i.e. aptamer chain in a flexible form) (through the π-π stacking interaction between the puric and pyimidic bases of nucleic acid aptamers and the graphene plane) while repelling the adsorption of the folded aptamer (i.e. aptamer in a rigid three-dimensional structure) (Liu et al., 2012b; Park et al., 2014). The marriage of graphene and aptamers enables people to create many ingenious strategies for aptasensing applications. A variety of proof-of-concept aptasensors based on graphene have been designed (Fig. 1). Aptasensors based on other two-dimensional nanomaterials, such as transition metal chalcogenides and metal oxides, are also included below.

Fig. 1

2. Surface functionalization strategies for two-dimensional nanomaterials-based aptasensors

One of the key considerations for the fabrication of an aptasensor is the immobilization of aptamers onto the surface of transducer, as the basis of the detection of the target molecule relies on its interaction with the former. For the inert graphitic structure, a pre-functionalization step is necessary prior to biomolecule immobilization. The currently developed strategies for graphene functionalization include covalent and non-covalent approaches. Conventional covalent treatments often include an oxidative functionalization that may damage graphene properties. Non-covalent approach relies mainly on π-π stacking interactions.

2.1. Non-covalent functionalization strategies

The non-covalent approach enables modifying graphene with desired functional groups, without affecting its intrinsic properties. Physical adsorption is the simplest immobilization method in the graphene-based aptasensors in view of the favorable feature of π-π stacking interaction between the puric and pyrimidic bases of aptamers and the hexagonal cells of graphene (Park et al., 2012). Du et al. used a graphene modified electrode to bind aptamer by physical adsorption (Du et al., 2012a). The recognition of the target protein in the solution led to a neutralization of the negatively charged phosphate backbone of the aptamer, resulting in the decrease of the electrochemical signals of cationic ruthenium complex. Another procedure for non-covalent functionalization relies on the use of polyaromatic hydrocarbons that strongly adsorb on graphene through π-π stacking interaction (Sun et al., 2013). The use of pyrene butyric acid for example, enables a stable and robust functionalization through π-π stacking of the four aromatic rings, while the terminal acid function remains free and available for further covalent grafting of biomolecules through their amine functions (Kong et al., 2013). This procedure offers the advantages of the covalent grafting without altering the graphitic properties.

Besides physical adsorption approach, electrostatic adsorption is another method in the assembly of aptamers onto transducers. The negatively charged aptamers can be electrostatically adsorbed onto positively charged transducers in neutral buffers of low

osmolarity (< 100 mM). By functionalization of graphene with charged materials, like poly(sodium 4-styrensulfonate) (Qin et al., 2012) and Fe_2O_3 (Du et al., 2013a), simple and label-free electrochemical aptasensors were constructed.

2.2. Covalent functionalization strategies

The covalent approach often relies on the oxidation of graphene. Indeed, graphene samples prepared by the oxidative methods or by the reduction of graphene oxide initially carry carbonyl and carboxyl functional groups (Biju, 2014). These groups can be coupled with biomolecules through their amine functions. Chemical oxidation of graphene enables increasing the density of carbonyl and carboxyl functional groups and is widely used for the chemical modification of the inert graphitic structure (Maiti et al., 2014). However, this procedure strongly affects the properties of graphene. The covalent modification of graphitic surface is also possible without a pre-oxidation step, through a free radical addition reaction, expected to have less impact on the electronic properties (Bekyarova et al., 2009). Besides the immobilization methods above, amide (Xiao et al., 2013) and phosphoramidate reactions (Liu et al., 2012a) were employed towards the fabrication of graphene-based aptasensors. In addition, some graphene derivatives, such as GO, were used as transducers in electrochemical aptasensors (Yan et al., 2013b).

2.3. Decoration with metal nanoparticles for immobilization

Graphene can be decorated with metal nanoparticles to enhance the signal of the transduction techniques or to increase the grafting area for aptamer immobilization (Rao et al., 2009). Gold nanoparticles (AuNPs) are the mostly founded metal nanoparticles in graphene-aptamer based biosensing system, since gold could form strong covalent bond (Au-S) with thiol group. An electrochemical aptasensor using graphene-AuNPs composite obtained by the reduction of tetrachloroauric acid with sodium citrate in a graphene water suspension was reported (Liang et al., 2011). In order to simplify the fabrication method, direct electrodeposition technique of AuNPs was also applied to electrochemical aptasensors. This method could produce graphene

transducers with a high-density of AuNPs that provide ultra-large specific surface area for aptamer immobilization (Jiang et al., 2012a). Most of graphene-based electrochemical aptasensors are constructed in this way, including probe-free and sandwich types. Recently, a simpler method to form graphene-AuNPs transducer by simultaneous electrodeposition of graphene and AuNPs onto the electrode surface was developed (Zheng et al., 2013). Two leukemia-type aptamers (sgc8c and KH1C12) were assembled on this transducer to capture the target cells and another layer of aptamers labeled with different redox tags were formed on the cell surface (Fig. 2a). By this strategy, they demonstrated an effective method for simultaneous detection of multiple leukemia-type cells.

Fig. 2

3. Transduction methods for two-dimensional nanomaterials-based aptasensors

3.1. Electrochemical aptasensors

Electrochemical methods have been extensively recognized as a powerful tool for fast access to (bio)chemical information in complex samples in view of their high sensitivity, fast response, easy operation, and low-cost. In a typical electrochemical aptasensing system, nucleic acid aptamers are immobilized on a conducting substrate (i.e., transducer). When binding to their target molecules, they fold their flexible chains into well-defined three-dimensional structures (Song et al., 2008). This behavior enables redox-active species-labeled aptamers to have a dynamic distance to the transducer (label type) or in solution to have a different steric hindrance in getting closer to the transducer (label-free type). Consequently, the formation of the aptamer-target complexes could be identified by probing the electron-transfer kinetics of the redox species.

3.1.1. As transducers in electrochemical aptasensors

Graphene-based electrochemical transducers have shown many excellent properties, such as wide electrochemical window, high signal/noise ratio, fast electron transfer kinetics, and more importantly the feasibility for composite incorporation,

which make them attractive platforms in electrochemical aptasensors (Chen et al., 2010; Huang et al., 2012; Ping et al., 2011). Table 1 summarizes the recent progress of graphene-based transducers for electrochemical aptasensors.

Table 1

Zhao et al. reported a graphene quantum dots (QDs)-based electrochemical aptasensor for the detection of thrombin, in which the aptamers were physically adsorbed onto graphene QDs surface and the redox specie $[Fe(CN)_6]^{3-/4-}$ was used as electrochemical probe (Zhao et al., 2011). By incorporation of redox-active species into the graphene-based transducer, probe-free detection was achieved. Additionally, a high-throughput and reusable aptasensing platform was established (Tang et al., 2011a) with magnetic graphene nanosheets as transducer. They further improved the detection system by coupling nuclease cleavage (DNase I) for signal amplification and distinguishable redox tag-conjugated aptamers for multiplex analysis (Fig. 2b) (Tang et al., 2011b).

Recently, the performance of various graphene materials, such as GO, electrochemically reduced graphene, and thermally reduced graphene was compared (Loo et al., 2012). Results showed that GO was the most sensitive platform for thrombin aptasensing. Furthermore, the different immobilization methods on the effect of impedance response of GO-based aptasensors were also studied (Loo et al., 2013a). It was discovered that while all three immobilization methods uniformly show a similar optimum amount of immobilized aptamer, physical and covalent immobilization methods exhibit higher selectivity than affinity immobilization.

3.1.2. As nanocarriers in electrochemical aptasensors

Another interesting application of graphene and its derivative in electrochemical aptasensors is to be used as a nanocarrier to load electroactive species, enzymes or recognition molecules (Table 2). As mentioned previously, graphene nanosheets have unusually large surface areas with the ability to incorporate various inorganic or organic species to build a multifunctional nanocarrier (Huang et al., 2012). That is,

graphene nanosheets could covalently attach or physically adsorb signal molecules and/or recognition elements on their surface. When using this nanocarrier to construct electrochemical aptasensors, it can significantly enlarge the loading of signal molecules and consequently increase the sensitivity. An electrochemical sandwich aptasensor for simultaneous detection of platelet-derived growth factor and thrombin was fabricated (Fig. 3a) (Bai et al., 2012b). Two graphene-based nanocarriers with different redox probes were synthesized and further used as the labels for aptamers through a sandwich assay in order to amplify the signals. Such an approach has demonstrated the capability of graphene-based nanocarriers to achieve a substantial amplification. GO was also used as nanocarrier in electrochemical aptasensors (Wang et al., 2012d). Chen et al. reported two simple probe-label-free electrochemical aptasensing strategies based on GO constructed nanocarriers (Chen et al., 2013).

Table 2

Fig. 3

3.1.3. Other electrochemical aptasensors

In addition to acting as transducers and nanocarriers in electrochemical aptasensors, graphene can also mediate electron-transfer in view of the high-density edge-plane-like defects present within its nanostructure (Ping et al., 2012). A label-free electrochemical aptasensor was constructed by taking advantage of the ultra-fast electron transfer ratio of graphene (Wang et al., 2012a). In the absence of target, aptamers immobilized on the gold electrode would adsorb graphene nanosheets due to the strong π-π interaction that accelerate the electron transfer ratio between the electroactive species and the electrode surface. In the presence of target, the binding reaction would inhibit the adsorption of graphene and block electron transfer. Yan et al. further improved this detection strategy by nuclease cleavage-assisted target recycling amplification yielding a detection limit of 0.065 pM for interferon-gamma (Yan et al., 2013a). Pumera's group employed graphene oxide nanoplatelets (GONPs)

as inherently electroactive labels for thrombin detection (Loo et al., 2013b). Their design consisted of GONPs with a dimension of 50 × 50 nm which has a reduction peak near ~1.2 V that can be used as an analytical signal. The different affinity of GONPs to unbound aptamers versus target-bound aptamers enabled GONPs to be utilized as an effective label for sensitive detection of thrombin (Fig. 3b).

3.2. Optical aptasensors

Optical aptasensing assays have been extensively used in medical diagnosis and environmental monitoring, due to their high sensitivity and simple readout devices (Chen et al., 2011; Wang et al., 2010a). The introduction of two-dimensional nanomaterials into optical aptasensors could eliminate the separation step and improve analytical performance since the two-dimensional nanostructures possess unique plane structure and optical properties (Du et al., 2013b). Recent studies on two-dimensional nanostructures-based optical aptasensors mainly focus on fluorescence and chemluminescence. Although GO is the most widely studied nanomaterial in optical aptasensing assays, other two-dimensional nanomaterials are also attracting attention, such as single-layer molybdenum sulfide (MoS_2) and carbon nitride nanosheet (CNNS).

3.2.1. Fluorescent aptasensors

Fluorescence is a commonly used signal transducing mechanism in aptamer-based assays in view of its sensitivity, and convenience. Since the aptamers can be easily labeled with various fluorophores (such as organic dyes and nanomaterials), approaches have focused on how to detect the changes of fluorescence intensity in response to target-aptamer binding (Wang et al., 2011b). Until now, there are two commonly used detection modes in fluorescent aptasensors, i.e. detection based on the change of fluorescent intensity (quenching or restoring of fluorescent molecules) and detection based on the change of fluorescent anisotropy (aka fluorescent polarization).

Sensing by change in fluorescent intensity

Fluorescence resonance energy transfer (FRET) is a nonradiative process in which a donor within excited state transfers energy to a proximal acceptor within a ground state and is commonly found in optical aptasensors (Zhang et al., 2013b). In a well-designed FRET-based aptasensing mode, the fluorophore (i.e. electron donor) and quencher (i.e. electron acceptor) are brought into proper distance from each other exclusively via the binding process. The low FRET efficiency and R^{-6} response dependence of the FRET fluorophore-quencher molecules requires careful design to avoid large background signals (Citartan et al., 2012). Two-dimensional nanomaterials may overcome these design limitations in view of their excellent fluorescence-quenching capability by intrasheet energy or electron-transfer. GO is commonly employed in FRET-based aptasensor designs with many advantages (Chen et al., 2012b). GO's hydrophilic nature and water miscibility facilitates homogeneous fluorescent signals. As an electron acceptor, GO can be employed as a generic quencher for numerous fluorophores, including organic dyes, conjugated polymers, and quantum dots. The quenching by GO is through long range resonance energy transfer (LrRET) which has R^{-4} dependence from the fluorophore (Liu et al., 2013a). Much like graphene, GO varies its response in regards to unfolded versus folded aptamers (i.e. upon binding to a target, a change in the aptamer tertiary structure will allow changes in fluorescent intensity). Such a design allows multiplexed FRET analysis towards multiple labeled aptamers on single GO sheet. Furthermore, with GO's inherent steric-hindrance, biomolecules may be protected from enzymatic degradation. Various GO-based FRET aptasensing assays are listed in Table 3.

Table 3

In a typical GO-based FRET aptasensing mode, aptamer firstly adsorbs onto the surface of GO and the labeled fluorophore is quenched by the GO (Fig. 4a). The binding reaction induces a conformational change of aptamer that enables the aptamer-target conjugate to dissociate from the GO and consequently the fluorescence of fluorophore is restored (Chang et al., 2010). Various fluorescent species, including

organic dyes and quantum dots, have been used in this sensing mode to detect small molecules and proteins (Dong et al., 2010). Huang et al. have carefully studied the effect of solution pH on the adsorption of aptamer to GO and the binding of aptamer to its target (Huang et al., 2011). They found these two processes could be controlled by tuning the solution pH. That means GO/aptamer based FRET sensing system could be easily restored.

Fig. 4

In order to improve sensitivity, several amplification strategies were explored. One effective method is to incorporate the nucleic acid-related enzymes into the detection process. As mentioned above, GO can protect the adsorbed aptamer from the enzymatic digestion. Inspired by this, deoxyribonuclease I (DNase I) was used to cleave the unadsorbed aptamer (Fig. 4b) (Lu et al., 2010). A much lower detection limit (40 nM) was achieved for the ATP detection which was ~250-fold lower than that of the strategy without DNase I (10 μM). Exonuclease III (Exo III), a double-stranded specific enzyme, was also used to amplify the fluorescent signal in GO-based FRET sensing (Chen et al., 2012a). Besides these nucleic acid lyases, Hu et al. employed polymerase Klenow fragment induced strand-displacement polymerization reaction to realize the highly sensitive detection of interferon-gamma (Fig. 4c) at a quite low detection limit of 1.5 fM (Hu et al., 2013).

Another approach for sensitivity enhancement is to tuning the distance between the fluorophore and GO. GO is an excellent quencher with an effective quenching distance of R^{-4} dependence that enables LrRET in the sensing process (Zhuang et al., 2013). Ueno et al. used a DNA spacer modified on aptamer to control the distance between the fluorophore and GO (Ueno et al., 2013). By carefully screening the length of spacer, a detection limit of ~1 nM for thrombin was obtained. Zhuang et al. employed LrRET as the signal transducing mechanism to detect cellular prion protein with a detection limit of 0.309 μg mL^{-1} (Zhuang et al., 2013).

An important issue in GO-based aptasensing is the multiplexed detection.

GO-based aptamer logic gates for simultaneous detection of ATP and thrombin was developed (Wang et al., 2012b). A paper-based microfluidic biochip integrated with GO and aptamer for fluorescent detection of two infectious pathogens was also developed (Zuo et al., 2013). Recently, a highly tunable GO microarray has been devised for high-throughput multiplexed protein sensing (Fig. 5) (Jung et al., 2013). A thin GO film building from layer-by-layer assemble technique was used as an excellent quencher of dye-labeled aptamers. By optimizing the layers of the GO film and constructing a microarray, four different targets could be detected simultaneously.

Fig. 5

Besides being a quencher, GO could be used as a fluorescent specie (i.e. electron donor) in FRET-based aptasensors. Shi et al. fabricated a fluorescent aptasensor based on a structure switchable aptamer, GNPs, and GO for the detection of cocaine (Shi et al., 2013). In the presence of cocaine, its corresponding aptamer folds into a three-way junction that shortens the distance of donor (GO) and acceptor (GNPs) resulting in the decrease of fluorescent intensity of the GO. In another work, a thymine-rich aptamer with a GO-based fluorophore was used to detect Hg^{2+} (Li et al., 2013a). The thymine-rich aptamer can bind with Hg^{2+} due to the formation of the thymine-Hg^{2+}-thymine complex, which brings the Hg^{2+} near the GO surface. If these mercury ions are close enough, they quench the fluorescence of GO through electron transfer from GO along the duplex DNA channel.

Other two-dimensional nanomaterials were also employed into FRET-based aptasensors. Single-layer MoS_2 possesses high fluorescence-quenching capability and exhibits different interaction toward unfolded and folded ssDNA (Zhu et al., 2013a). Fluorophore labeled aptamer was mixed with target and then MoS_2 was subsequently added. The poor affinity between MoS_2 nanosheets and aptamer-target conjugates resulted in no loss of fluorescence and a quantitative readout for the target (adenosine) was possible with a detection limit of 5 μM. Ge et al. extended this nanomaterials-based FRET to thrombin target (Fig. 6a) (Ge et al., 2014). Manganese

dioxide (MnO_2) nanosheets could also be used as an effective energy acceptor. Yuan et al. fabricated two aptasensors for the homogeneous analysis of ochratoxin A and cathepsin D based on the MnO_2 nanosheets acting as nanoquencher and upconversion phosphors labeled aptamers acting as bioprobes (Fig. 6b) (Yuan et al., 2014).

Fig. 6

In addition to the FRET-based detection mode, other signal transducing mechanisms were also introduced into the sensing by the change of fluorescence intensity. Wu's group reported a 'turn-on' fluorescent aptasensor through nano-metal surface energy transfer (NSET) from CdSe/ZnS QDs to GO (Li et al., 2013b). NSET typically possesses a longer energy transfer distance than FRET and does not need a resonant interaction between the electrons but rather an interband electronic transition. Based on this fluorescent quenching mechanism, a lower detection limit of 90 pM was obtained for Pb^{2+} detection. Another fluorescent quenching mechanism is based on the photoinduced electron transfer (PET) process. Recently, Wang et al. developed a carbon nitrite nanosheet (CNNS)-based fluorescent aptasensor for Hg^{2+} detection (Wang et al., 2013a). They found the fluorescence quenching followed a static quenching through the PET from the excited fluorophore to the conductive band of CNNS. As a result, a detection limit of 16 nM for Hg^{2+} detection was achieved.

Sensing by change in fluorescent anisotropy

Fluorescence anisotropy (FA) is another fluorescent signal transducing method that provides information about the molecular mobility, orientation, and interaction process through changes in the molecular weight of the fluorescent species (Liu et al., 2013c). It is a well-documented method to detect biologically related macromolecules by coupling with dye-labeled aptamers (Gokulrangan et al., 2005). However, it is hard to detect small molecule targets as changes in low molecular mass cannot produce appropriate changes in observable anisotropy (Zhang et al., 2011a). To address this issue, Liu et al. developed an aptasensing strategy based on FA signal amplification by using GO as the signal amplifier (Liu et al., 2013b). Fig. 7 shows two strategies of

GO-based FA detection. For the FA reduction assay ('signal off' mode), a fluorescein labeled aptamer adsorbs on the surface of GO, where its rotation is constrained resulting in a high fluorescence anisotropy. In the presence of target, the structure change of aptamer induces desorption of aptamer from GO and a subsequent decrease of FA. While in the 'signal on' mode (FA enhancement assay), a fluorescent dye-labeled complementary ssDNA to aptamer (that could form a dsDNA with low anisotropy signal) is used as a signaling probe. When displaced by the target, the released ssDNA is adsorbed onto the surface of GO inducing an increase in the anisotropy value. By this approach, they demonstrated a sensitive aptasensor for ATP detection. A similar FA transducing strategy for copper ion detection was also developed (Yu et al., 2013a).

Fig. 7

3.2.2. Chemiluminescent aptasensors

Chemiluminescent (CL) detection has been widely used in various fields, due to its sensitive, simple, and inexpensive characteristics (Cho et al., 2014). Compared to the fluorescence, it does not require an external light source, and the life time of the luminescence species is much longer than that of fluorescent ones. Taking advantage of this method, a CL detection system was established on the basis of the excellent luminescence quenching capability of GO through chemiluminescent resonance energy transfer (CRET) and the interaction of unfolded aptamer with GO (Choi and Lee, 2013). Furthermore, by introduction of magnetic beads (Fe_3O_4) on GO nanosheets, the impurities in human serum samples capable of reducing the efficiency of the aptasensor were removed and rapid detection of prostate specific protein was realized. A label-free CL aptasensor for ATP detection was developed (Song et al., 2014), in which a CL reagent phenylgyoxal was used as the signal reporter that could react specifically with guanine bases of aptamer adsorbed on the GO surface. The presence of ATP would release the aptamer from GO nanosheets that induce the decrease of the CL signal.

Electrogenerated chemiluminescence (ECL) is another effective detection method in aptasensing due to the combination of the electrochemical advantages with CL sensitivity (Wang et al., 2013b; Zhou et al., 2013). Like graphene-based electrochemical aptasensors, graphene also could be used as transducer and nanocarrier in ECL aptasensors with enhanced performance (Gan et al., 2012; Liao et al., 2011; Xie et al., 2013; Yu et al., 2013b). Recently, Wei et al. developed a sensitive aptasensor for the detection of mucin 1 protein and MCF-7 cells based on ECL resonance energy transfer from a ruthenium complex to GO (Wei et al., 2012). Jin et al. reported a GO-based ECL detection approach using an iridium complex as the ECL reagent (Jin et al., 2013). An interesting ECL system using graphene QDs was explored to detect ATP (Lu et al., 2013). Graphene QDs exhibit bright blue emission under ultraviolet irradiation and could combine with H_2O_2 as a coreactant in ECL detection. By employing SiO_2 nanospheres as a signal carrier, a sensitive aptasensor for the detection of ATP was constructed through a SiO_2/Graphene QDs-based ECL signal amplification strategy.

3.3 Other transduction techniques for two-dimensional nanomaterials-based aptasensors

Besides the electrochemical and optical transducing mechanisms mentioned previously, a number of other transducing mechanisms have been proposed in two-dimensional nanomaterials-based aptasensors. Electronic detection based on field-effect transistor (FET) is an effective method (Willner and Zayats, 2007). Graphene-based FET has shown great potential for the sensitive determination of various analytes (He et al., 2012a; Liu et al., 2012b). In a typical graphene-based FET sensing system, graphene sheets were coated on a Si/SiO_2 substrate to obtain a channel (Ohno et al., 2010). Then a small organic molecule (1-pyrenebutanoic acid succinimidyl ester) was used as a linker to attach the aptamer onto the graphene sheet. The binding reaction between aptamer and target can induce an effect on the charge-carrier density on the surface of the graphene plane, and consequently it may

allow label-free detection of analytes. One key factor in the design of a FET aptasensor is to ensure the binding reaction of aptamer-ligand occurs within the Debye length since the charge change in the area outside the Debye length cannot induce the carriers change of graphene (Ohno et al., 2010). Graphene nanosheets made from mechanical exfoliation and chemical reduction have been used to fabricate FETs for aptasensing IgE, thrombin, and cocaine (Ohno et al., 2010 and 2011). A FET based on polypyrrole-converted nitrogen-doped few-layer graphene was developed (Kwon et al., 2012). By doping the graphene planar lattice with nitrogen atoms, the band gap of graphene was opened and consequently a stable *n*-type (electron-transporting) behavior was observed (Fig. 8a). A sandwich-type graphene-based FET was reported (Kim et al., 2013), in which secondary aptamer-conjugated gold nanoparticles was used to increase the charge-doping in graphene channel (Fig. 8b) and a ultra-low detection limit of 1.2 aM for a protective antigen was obtained in that detection mode. A graphene-based FET aptasensor based on aptazyme modified AuNPs for the detection of Pb^{2+} with a detection limit at the nM level was developed (Wen et al., 2013). Surface plasmon resonance (SPR) is another transducing mechanism in graphene-based aptasensors (Subramanian et al., 2013). A SPR aptasensing platform based on graphene film for thrombin detection was recently reported (Wang et al., 2011a). Prior to the detection, graphene sheets were assembled on a positively charged SPR gold film via electrostatic interaction and the target aptamer was noncovalently adsorbed onto the graphene sheets (Fig. 8c). The binding reaction between the aptamer and target would greatly disturb the interaction between the aptamer and graphene that took off the aptamer from the graphene surface resulting in a decreased SPR angle. Finally, Zhang et al. recently developed a quartz crystal microbalance aptasensor for thrombin detection based on an amino-functionalized nanocomposite of graphene and plasma-polymerized allylamine (Zhang et al., 2014). They found that the presence of graphene enhances the electrochemical activity of the plasma and improves the sensitivity of the resulting

aptasensor, opening a promising use of these materials in piezoelectric transduction.

Fig. 8

4. Conclusions

This work has presented an overview about current advances in the development and application of two-dimensional nanomaterials-based aptasensors. Different types of two-dimensional nanomaterials have been employed to explore aptasensors with a range of signal transducing mechanisms, such as electrochemical, optical, and so on. Significantly, some reagent-free and one-step analysis strategies have been established by the assembly of two-dimensional nanostructures with aptamers. However, despite these advances, graphene and graphene-like two-dimensional nanomaterials-based aptasensors are still relatively immature in development compared to other biosensing tools. Many technical hurdles still need to be addressed, including the desorption of bioelements and nanomaterials from the aptasensing devices over time, the effect of non-uniform two-dimensional nanomaterials (i.e. due to shifts in nanomaterial size or shape) on performance of aptasensing devices, and the low affinity and specificity of aptamers towards inorganic small molecules.

Additionally, some important issues and challenges should be prioritized. Current studies are mainly on graphene and its derivative-based aptasensors. Recently, other two-dimensional nanomaterials with unique features have been synthesized. For example, recent studies have shown that single-layer MoS_2 constructed FET displays a room-temperature On/Off ratio exceeding 10^8 (Wang et al., 2012c). That would help MoS_2 two-dimensional nanomaterials in the construction of high-performance FET aptasensors (Huang et al., 2013). On the other hand, the analytes of aptasensors should be diversified, not limited to thrombin and ATP even they are important in biology. Almost all of the current two-dimensional nanomaterials-based aptasensors use DNA aptamers as the molecular recognition element. The reports on combination of RNA aptamers with two-dimensional nanomaterials constructed aptasensors are rarely found, probably due to their expensive synthesis and inherent instability.

Nevertheless, RNA aptamers have higher affinity towards their targets than DNA aptamers. They also show more abundant structural information changes upon binding that enables more sensitive and simpler aptasensing strategies (Patel et al., 1997).

An important challenge of two-dimensional nanomaterials-based aptasensors is the practical application, i.e. analysis of analytes in real world, complex environments. Two main issues should be considered in this context. One is the sample matrix effect, since the real sample (e.g. body fluids, wastewater) always contain a mixture of macromolecules, ions, and particles that would induce a nonspecific signal in the detection process. Therefore, research work focusing on aptasensors should explore the feasibility of aptasensors and their recognition limits in complex environments. Typically, most reported results were performed in optimal laboratory conditions. The last issue is scalable methods of fabrication. Most fabrication techniques for aptasensors are designed for fast production at laboratory scales and are unable to be scaled for rapid production. If aptasensors are to be routinely commercialized, ubiquitous, scalable methods of synthesis need to be developed to produce greater amounts of aptasensors that are ISO compliant, have reproducible specifications, and can be made from cheap starting materials. Such a technique is the prerequisite for the successful commercial application of any aptasensing devices. Nevertheless, we expect that these two-dimensional nanomaterials-based aptasensing devices will eventually become an effectively routine analysis tool that could meet various challenges.

Acknowledgements

This Research is conducted by NTU-HUJ-BGU Nanomaterials for Energy and Water Management Programme under the Campus for Research Excellence and Technological Enterprise (CREATE), that is supported by the National Research Foundation, Prime Minister's Office, Singapore. Funding was also greatly appreciated from the Ministry of Education Tier 1 Grants: RG46/11, RG54/13, and Tier 2 grant:

MOE2012-T2-2-046.

References

Amaya-Gonzalez, S., de-los-Santos-Alvarez, N., Miranda-Ordieres, A.J., Lobo-Castanon, M.J., 2013. Sensors 13, 16292-16311.

Bai, L.J., Yan, B., Chai, Y.Q., Yuan, R., Yuan, Y.L., Xie, S.B., Jiang, L.P., He, Y., 2013. Analyst 138, 6595-6599.

Bai, L.J., Yuan, R., Chai, Y.Q., Yuan, Y.L., Wang, Y., Xie, S.B., 2012a. Chem. Commun. 48, 10972-10974.

Bai, L.J., Yuan, R., Chai, Y.Q., Zhuo, Y., Yuan, Y.L., Wang, Y., 2012b. Biomaterials 33, 1090-1096.

Balandin, A.A., 2011. Nat. Mater. 10, 569-581.

Bekyarova, E., Itkis, M.E., Ramesh, P., Berger, C., Sprinkle, M., de Heer, W.A., Haddon, R.C., 2009. J. Am. Chem. Soc. 131, 1336-1337.

Biju, V. 2014. Chem. Soc. Rev. 43, 744-764.

Chang, H.X., Tang, L.H., Wang, Y., Jiang, J.H., Li, J.H., 2010. Anal. Chem. 82, 2341-2346.

Chen, C.F., Zhao, J.J., Jiang, J.H., Yu, R.Q., 2012a. Talanta 101, 357-361.

Chen, D., Feng, H.B., Li, J.H., 2012b. Chem. Rev. 112, 6027-6053.

Chen, D., Tang, L.H., Li, J.H., 2010. Chem. Soc. Rev. 39, 3157-3180.

Chen, J.R., Jiao, X.X., Luo, H.Q., Li, N.B., 2013. J. Mater. Chem. B 1, 861-864.

Chen, T., Shukoor, M.I., Chen, Y., Yuan, Q.A., Zhu, Z., Zhao, Z.L., Gulbakan, B., Tan, W.H., 2011. Nanoscale 3, 546-556.

Cho, S., Park, L., Chong, R., Kim, Y.T., Lee, J.H., 2014. Biosens. Bioelectron. 52, 310-316.

Choi, H.K., Lee, J.H., 2013. Anal. Methods 5, 6964-6968.

Citartan, M., Gopinath, S.C.B., Tominaga, J., Tan, S.C., Tang, T.H., 2012. Biosens. Bioelectron. 34, 1-11.

Craciun, M.F., Russo, S., Yamamoto, M., Tarucha, S., 2011. Nano Today 6, 42-60.

Deng, K., Xiang, Y., Zhang, L.Q., Chen, Q.H., Fu, W.L., 2013. Anal. Chim. Acta 759, 61-65.

Dong, H.F., Gao, W.C., Yan, F., Ji, H.X., Ju, H.X., 2010. Anal. Chem. 82, 5511-5517.

Du, M., Yang, T., Guo, X.H., Zhong, L., Jiao, K., 2013a. Talanta 105, 229-234.

Du, M., Yang, T., Zhao, C.Z., Jiao, K., 2012a. Sens. Actuators, B 169, 255-260.

Du, Y., Guo, S.J., Qin, H.X., Dong, S.J., Wang, E.K., 2012b. Chem. Commun. 48, 799-801.

Du, Y., Li, B.L., Wang, E.K., 2013b. Acc. Chem. Res. 46, 203-213.

Ellington, A.D., Szostak, J.W., 1990. Nature 346, 818-822.

Famulok, M., Mayer, G., 2011. Acc. Chem. Res. 44, 1349-1358.

Feng, L.Y., Chen, Y., Ren, J.S., Qu, X.G., 2011. Biomaterials 32, 2930-2937.

Gan, X.X., Yuan, R., Chai, Y.Q., Yuan, Y.L., Cao, Y.L., Liao, Y.H., Liu, H.J., 2012. Anal. Chim. Acta 726, 67-72.

Ge, J., Ou, E.C., Yu, R.Q., Chu, X., 2014. J. Mater. Chem. B 2, 625-628.
Geim, A.K., Grigorieva, I.V., 2013. Nature 499, 419-425.
Georgakilas, V., Otyepka, M., Bourlinos, A.B., Chandra, V., Kim, N., Kemp, K.C., Hobza, P., Zboril, R., Kim, K.S., 2012. Chem. Rev. 112, 6156-6214.
Gokulrangan, G., Unruh, J.R., Holub, D.F., Ingram, B., Johnson, C.K., Wilson, G.S., 2005. Anal. Chem. 77, 1963-1970.
Govindaraju, T., Avinash, M.B., 2012. Nanoscale 4, 6102-6117.
Guo, Y.J., Han, Y.J., Guo, Y.X., Dong, C., 2013. Biosens. Bioelectron. 45, 95-101.
Han, J., Zhuo, Y., Chai, Y.Q., Yuan, R., Xiang, Y., Zhu, Q., Liao, N., 2013. Biosens. Bioelectron. 46, 74-79.
He, Q.Y., Wu, S.X., Yin, Z.Y., Zhang, H., 2012a. Chem. Sci. 3, 1764-1772.
He, Y., Lin, Y., Tang, H.W., Pang, D.W., 2012b. Nanoscale 4, 2054-2059.
He, Y., Wang, Z.G., Tang, H.W., Pang, D.W., 2011. Biosens. Bioelectron. 29, 76-81.
Hong, P., Li, W.L., Li, J.M., 2012. Sensors 12, 1181-1193.
Hu, K., Liu, J.W., Chen, J., Huang, Y., Zhao, S.L., Tian, J.N., Zhang, G.H., 2013. Biosens. Bioelectron. 42, 598-602.
Hu, P., Zhu, C.Z., Jin, L.H., Dong, S.J., 2012. Biosens. Bioelectron. 34, 83-87.
Huang, P.J.J., Kempaiah, R., Liu, J.W., 2011. J. Mater. Chem. 21, 8991-8993.
Huang, X., Qi, X.Y., Boey, F., Zhang, H., 2012. Chem. Soc. Rev. 41, 666-686.
Huang, X., Zeng, Z.Y., Zhang, H., 2013. Chem. Soc. Rev. 42, 1934-1946.
Jiang, B.Y., Wang, M., Chen, Y., Xie, J.Q., Xiang, Y., 2012a. Biosens. Bioelectron. 32, 305-308.
Jiang, L.P., Yuan, R., Chai, Y.Q., Yuan, Y.L., Bai, L.J., Wang, Y., 2012b. Analyst 137, 2415-2420.
Jin, G.X., Lu, L.J., Gao, X.Y., Li, M.J., Qiu, B., Lin, Z.Y., Yang, H.H., Chen, G.N., 2013. Electrochim. Acta 89, 13-17.
Jung, Y.K., Lee, T., Shin, E., Kim, B.S., 2013. Sci. Rep. 3, 3367.
Kim, D.J., Park, H.C., Sohn, I.Y., Jung, J.H., Yoon, O.J., Park, J.S., Yoon, M.Y., Lee, N.E., 2013. Small 9, 3352-3360.
Kong, N., Huang, X.D., Cui, L., Liu, J.Q., 2013. Sci. Adv. Mater. 5, 1083-1089.
Koski, K.J., Cui, Y., 2013. ACS Nano 7, 3739-3743.
Kuila, T., Bose, S., Khanra, P., Mishra, A.K., Kim, N.H., Lee, J.H., 2011. Biosens. Bioelectron. 26, 4637-4648.
Kwon, O.S., Park, S.J., Hong, J.Y., Han, A.R., Lee, J.S., Lee, J.S., Oh, J.H., Jang, J., 2012. ACS Nano 6, 1486-1493.
Leonard, F., Talin, A.A., 2011. Nat. Nanotechnol. 6, 773-783.
Li, D., Song, S.P., Fan, C.H., 2010. Acc. Chem. Res. 43, 631-641.
Li, M., Zhou, X.J., Ding, W.Q., Guo, S.W., Wu, N.Q., 2013a. Biosens. Bioelectron. 41, 889-893.
Li, M., Zhou, X.J., Guo, S.W., Wu, N.Q., 2013b. Biosens. Bioelectron. 43, 69-74.

Li, X.M., Song, J., Wang, Y., Cheng, T., 2013c. Anal. Chim. Acta 797, 95-101.
Liang, J.F., Chen, Z.B., Guo, L., Li, L.D., 2011. Chem. Commun. 47, 5476-5478.
Liang, J.F., Wei, R., He, S., Liu, Y.K., Guo, L., Li, L.D., 2013. Analyst 138, 1726-1732.
Liao, Y.H., Yuan, R., Chai, Y.Q., Mao, L., Zhuo, Y., Yuan, Y.L., Bai, L.J., Yuan, S.R., 2011. Sens. Actuators, B 158, 393-399.
Lim, Y.C., Kouzani, A.Z., Duan, W., 2010. J. Biomed. Nanotechnol. 6, 93-105.
Liu, B.W., Sun, Z.Y., Zhang, X., Liu, J.W., 2013a. Anal. Chem. 85, 7987-7993.
Liu, F., Zhang, Y., Yu, J.H., Wang, S.W., Ge, S.G., Song, X.R., 2014. Biosens. Bioelectron. 51, 413-420.
Liu, J.H., Wang, C.Y., Jiang, Y., Hu, Y.P., Li, J.S., Yang, S., Li, Y.H., Yang, R.H., Tan, W.H., Huang, C.Z., 2013b. Anal. Chem. 85, 1424-1430.
Liu, J.W., Cao, Z.H., Lu, Y., 2009. Chem. Rev. 109, 1948-1998.
Liu, Q.Y., Xu, X.J., Zhang, L.N., Luo, X.D., Liang, Y., 2013c. Analyst 138, 2661-2668.
Liu, S., Xing, X.R., Yu, J.H., Lian, W.J., Li, J., Cui, M., Huang, J.D., 2012a. Biosens. Bioelectron. 36, 186-191.
Liu, Y.X., Dong, X.C., Chen, P., 2012b. Chem. Soc. Rev. 41, 2283-2307.
Loo, A.H., Bonanni, A., Pumera, M., 2012. Nanoscale 4, 143-147.
Loo, A.H., Bonanni, A., Pumera, M., 2013a. Chem. Asian J. 8, 198-203.
Loo, A.H., Bonanni, A., Pumera, M., 2013b. Nanoscale 5, 4758-4762.
Lu, C.H., Li, J.A., Lin, M.H., Wang, Y.W., Yang, H.H., Chen, X., Chen, G.N., 2010. Angew. Chem. Int. Ed. 49, 8454-8457.
Lu, J.J., Yan, M., Ge, L., Ge, S.G., Wang, S.W., Yan, J.X., Yu, J.H., 2013. Biosens. Bioelectron. 47, 271-277.
Lubin, A.A., Plaxco, K.W., 2010. Acc. Chem. Res. 43, 496-505.
Maiti, U.N., Lee, W.J., Lee, J.M., Oh, Y., Kim, J.Y., Kim, J.E., Shim, J., Han, T.H., Kim, S.O., 2014. Adv. Mater. 26, 40-67.
Mao, H.Y., Laurent, S., Chen, W., Akhavan, O., Imani, M., Ashkarran, A.A., Mahmoudi, M., 2013. Chem. Rev. 113, 3407-3424.
Meir, A., Stojanovic, M., Marks, R.S., 2007. Aptameric Biosensors, in: Marks, R.S., Cullen, D., Lowe, C., Weetall H.H., Karube I., (Eds), Handbook of Biosensors and Biochips. John Wiley & Sons Ltd Publishers, pp. 217-232.
Novoselov, K.S., Geim, A.K., Morozov, S.V., Jiang, D., Zhang, Y., Dubonos, S.V., Grigorieva, I.V., Firsov, A.A., 2004. Science 306, 666-669.
Ohno, Y., Maehashi, K., Inoue, K., Matsumoto, K., 2011. Jpn. J. Appl. Phys. 50, 070120.
Ohno, Y., Maehashi, K., Matsumoto, K., 2010. J. Am. Chem. Soc. 132, 18012-18013.
Park, J.W., Lee, S.J., Choi, E.J., Kim, J., Song, J.Y., Gu, M.B., 2014. Biosens. Bioelectron. 51, 324-329.

671 Park, J.W., Tatavarty, R., Kim, D.W., Jung, H.T., Gu, M.B., 2012. Chem. Commun. 48, 2071-2073.
672 Park, S., Ruoff, R.S., 2009. Nat. Nanotechnol. 4, 217-224.
673 Patel, D.J., Suri, A.K., Jiang, F., Jiang, L.C., Fan, P., Kumar, R.A., Nonin, S., 1997. J. Mol. Biol. 272,
674 645-664.
675 Peng, K.F., Zhao, H.W., Wu, X.F., Yuan, Y.L., Yuan, R., 2012. Sens. Actuators, B 169, 88-95.
676 Ping, J.F., Wang, Y.X., Fan, K., Wu, J., Ying, Y.B., 2011. Biosens. Bioelectron. 28, 204-209.
677 Ping, J.F., Wu, J., Wang, Y.X., Ying, Y.B., 2012. Biosens. Bioelectron. 34, 70-76.
678 Pu, W.D., Zhang, L., Huang, C.Z., 2012. Anal. Methods 4, 1662-1666.
679 Pu, Y., Zhu, Z., Han, D., Liu, H.X., Liu, J., Liao, J., Zhang, K.J., Tan, W.H., 2011. Analyst 136,
680 4138-4140.
681 Qi, C., Bing, T., Mei, H.C., Yang, X.J., Liu, X.J., Shangguan, D.H., 2013. Biosens. Bioelectron. 41,
682 157-162.
683 Qin, H.X., Liu, J.Y., Chen, C.G., Wang, J.H., Wang, E.K., 2012. Anal. Chim. Acta 712, 127-131.
684 Qiu, L., Zhou, H., Zhu, W.P., Qiu, L.P., Jiang, J.H., Shen, G.L., Yu, R.Q., 2013. New J. Chem. 37,
685 3998-4003.
686 Rao, C.N.R., Sood, A.K., Subrahmanyam, K.S., Govindaraj, A., 2009. Angew. Chem. Int. Ed. 48,
687 7752-7777.
688 Robertson, D.L., Joyce, G.F., 1990. Nature 344, 467-468.
689 Sheng, L.F., Ren, J.T., Miao, Y.Q., Wang, J.H., Wang, E.K., 2011. Biosens. Bioelectron. 26, 3494-3499.
690 Shi, Y., Dai, H.C., Sun, Y.J., Hu, J.T., Ni, P.J., Li, Z., 2013. Analyst 138, 7152-7156.
691 Song, S.P., Wang, L.H., Li, J., Zhao, J.L., Fan, C.H., 2008. Trends Anal. Chem. 27, 108-117.
692 Song, W., Li, H., Liu, H.P., Wu, Z.S., Qiang, W.B., Xu, D.K., 2013. Electrochem. Commun. 31, 16-19.
693 Song, Y.H., Yang, X., Li, Z.Q., Zhao, Y.J., Fan, A.P., 2014. Biosens. Bioelectron. 51, 232-237.
694 Subramanian, P., Lesniewski, A., Kaminska, I., Vlandas, A., Vasilescu, A., Niedziolka-Jonsson, J.,
695 Pichonat, E., Happy, H., Boukherroub, R., Szunerits, S., 2013. Biosens. Bioelectron. 50,
696 239-243.
697 Sun, T., Wang, L., Li, N., Gan, X.X., 2011a. Bioprocess Biosyst. Eng. 34, 1081-1085.
698 Sun, W.L., Shi, S., Yao, T.M., 2011b. Anal. Methods 3, 2472-2474.
699 Sun, Y.B., Yang, S.B., Zhao, G.X., Wang, Q., Wang, X.K., 2013. Chem. Asian J. 8, 2755-2761.
700 Tang, D.P., Tang, J., Li, Q.F., Liu, B.Q., Yang, H.H., Chen, G.N., 2011a. RSC Adv. 1, 40-43.
701 Tang, D.P., Tang, J., Li, Q.F., Su, B.L., Chen, G.N., 2011b. Anal. Chem. 83, 7255-7259.
702 Tuerk, C., Gold, L., 1990. Science 249, 505-510.
703 Ueno, Y., Furukawa, K., Matsuo, K., Inoue, S., Hayashi, K., Hibino, H., 2013. Chem. Commun. 49,
704 10346-10348.
705 Vinkenborg, J.L., Karnowski, N., Famulok, M., 2011. Nat. Chem. Biol. 7, 519-527.
706 Wang, G.Q., Wang, Y.Q., Chen, L.X., Choo, J., 2010a. Biosens. Bioelectron. 25, 1859-1868.
707 Wang, L., Xu, M., Han, L., Zhou, M., Zhu, C.Z., Dong, S.J., 2012a. Anal. Chem. 84, 7301-7307.

Wang, L., Zhu, C.Z., Han, L., Jin, L.H., Zhou, M., Dong, S.J., 2011a. Chem. Commun. 47, 7794-7796.

Wang, L., Zhu, J.B., Han, L., Jin, L.H., Zhu, C.Z., Wang, E.K., Dong, S.J., 2012b. ACS Nano 6, 6659-6666.

Wang, Q.B., Wang, W., Lei, J.P., Xu, N., Gao, F.L., Ju, H.X., 2013a. Anal. Chem. 85, 12182-12188.

Wang, Q.H., Kalantar-Zadeh, K., Kis, A., Coleman, J.N., Strano, M.S., 2012c. Nat. Nanotechnol. 7, 699-712.

Wang, R.E., Zhang, Y., Cai, J., Cai, W., Gao, T., 2011b. Curr. Med. Chem. 18, 4175-4184.

Wang, S.E., Si, S.H., 2013. Appl. Spectrosc. 67, 1270-1274.

Wang, X.Y., Gao, A., Lu, C.C., He, X.W., Yin, X.B., 2013b. Biosens. Bioelectron. 48, 120-125.

Wang, Y., Li, Z.H., Hu, D.H., Lin, C.T., Li, J.H., Lin, Y.H., 2010b. J. Am. Chem. Soc. 132, 9274-9276.

Wang, Y., Yuan, R., Chai, Y.Q., Yuan, Y.L., Bai, L.J., 2012d. Biosens. Bioelectron. 38, 50-54.

Wang, Y., Yuan, R., Chai, Y.Q., Yuan, Y.L., Bai, L.J., Liao, Y.H., 2011c. Biosens. Bioelectron. 30, 61-66.

Wang, Y.P., Xiao, Y.H., Ma, X.L., Lia, N., Yang, X.D., 2012e. Chem. Commun. 48, 738-740.

Wang, Y.X., Ye, Z.Z., Si, C.Y., Ying, Y.B., 2012f. Chin. J. Anal. Chem. 40, 634-642.

Wei, W., Li, D.F., Pan, X.H., Liu, S.Q., 2012. Analyst 137, 2101-2106.

Wen, Y.Q., Li, F.B.Y., Dong, X.C., Zhang, J., Xiong, Q.H., Chen, P., 2013. Adv. Healthcare Mater. 2, 271-274.

Willner, I., Zayats, M., 2007. Angew. Chem. Int. Ed. 46, 6408-6418.

Wu, J.S., Pisula, W., Mullen, K., 2007. Chem. Rev. 107, 718-747.

Wu, S.J., Duan, N., Ma, X.Y., Xia, Y., Wang, H.G., Wang, Z.P., Zhang, Q., 2012. Anal. Chem. 84, 6263-6270.

Xiao, Y.H., Wang, Y.P., Wu, M., Ma, X.L., Yang, X.D., 2013. J. Electroanal. Chem. 702, 49-55.

Xie, L.L., You, L.Q., Cao, X.Y., 2013. Spectrochim. Acta, Part A 109, 110-115.

Xie, S.B., Chai, Y.Q., Yuan, R., Bai, L.J., Yuan, Y.L., Wang, Y., 2012a. Anal. Chim. Acta 755, 46-53.

Xie, S.B., Yuan, R., Chai, Y.Q., Bai, L.J., Yuan, Y.L., Wang, Y., 2012b. Talanta 98, 7-13.

Xing, X.J., Liu, X.G., Yue, H., Luo, Q.Y., Tang, H.W., Pang, D.W., 2012. Biosens. Bioelectron. 37, 61-67.

Xu, M.S., Liang, T., Shi, M.M., Chen, H.Z., 2013a. Chem. Rev. 113, 3766-3798.

Xu, Z.H., He, C., Sun, T., Wang, L., 2013b. Electroanalysis 25, 2339-2344.

Yan, G.P., Wang, Y.H., He, X.X., Wang, K.M., Liu, J.Q., Du, Y.D., 2013a. Biosens. Bioelectron. 44, 57-63.

Yan, M., Sun, G.Q., Liu, F., Lu, J.J., Yu, J.H., Song, X.R., 2013b. Anal. Chim. Acta 798, 33-39.

Yang, W.R., Ratinac, K.R., Ringer, S.P., Thordarson, P., Gooding, J.J., Braet, F., 2010. Angew. Chem. Int. Ed. 49, 2114-2138.

Yu, Y., Liu, Y., Zhen, S.J., Huang, C.Z., 2013a. Chem. Commun. 49, 1942-1944.

Yu, Y.Q., Cao, Q., Zhou, M., Cui, H., 2013b. Biosens. Bioelectron. 43, 137-142.

745 Yuan, Y.L., Gou, X.X., Yuan, R., Chai, Y.Q., Zhuo, Y., Mao, L., Gan, X.X., 2011a. Biosens. Bioelectron.
746 26, 4236-4240.
747 Yuan, Y.L., Gou, X.X., Yuan, R., Chai, Y.Q., Zhuo, Y., Ye, Y., Gan, X.X., 2011b. Biosens. Bioelectron.
748 30, 123-127.
749 Yuan, Y.L., Liu, G.P., Yuan, R., Chai, Y.Q., Gan, X.X., Bai, L.J., 2013. Biosens. Bioelectron. 42,
750 474-480.
751 Yuan, Y.X., Wu, S.F., Shu, F., Liu, Z.H., 2014. Chem. Commun. 50, 1095-1097.
752 Zhang, D.D., Fu, L., Liao, L., Liu, N., Dai, B.Y., Zhang, C.X., 2012a. Nano Res. 5, 875-887.
753 Zhang, D.P., Lu, M.L., Wang, H.L., 2011a. J. Am. Chem. Soc. 133, 9188-9191.
754 Zhang, H.F., Han, Y.J., Guo, Y.J., Dong, C., 2012b. J. Mater. Chem. 22, 23900-23905.
755 Zhang, J., Chai, Y.Q., Yuan, R., Yuan, Y.L., Bai, L.J., Xie, S.B., 2013a. Analyst 138, 6938-6945.
756 Zhang, J.N., Liu, B., Liu, H.X., Zhang, X.B., Tan, W.H., 2013b. Nanomedicine 8, 983-993.
757 Zhang, P., Wang, Y., Leng, F., Xiong, Z.H., Huang, C.Z., 2013c. Talanta 112, 117-122.
758 Zhang, X.R., Li, S.G., Jin, X., Zhang, S.S., 2011b. Chem. Commun. 47, 4929-4931.
759 Zhang, Z., Luo, L.Q., Zhu, L.M., Ding, Y.P., Deng, D.M., Wang, Z.X., 2013d. Analyst 138, 5365-5370.
760 Zhang, Z.H., Liu, S.L., Shi, Y., Zhang, Y.C., Peacock, D., Yan, F.F., Wang, P.Y., He, L.H., Feng, X.Z.,
761 Fang, S.M., 2014. J. Mater. Chem. B 2, 1530-1538.
762 Zhao, J., Chen, G.F., Zhu, L., Li, G.X., 2011. Electrochem. Commun. 13, 31-33.
763 Zheng, T.T., Tan, T.T., Zhang, Q.F., Fu, J.J., Wu, J.J., Zhang, K., Zhu, J.J., Wang, H., 2013. Nanoscale 5,
764 10360-10368.
765 Zhou, H., Zhang, Y.Y., Liu, J., Xu, J.J., Chen, H.Y., 2013. Chem. Commun. 49, 2246-2248.
766 Zhou, J., Battig, M.R., Wang, Y., 2010. Anal. Bioanal.Chem. 398, 2471-2480.
767 Zhu, C.F., Zeng, Z.Y., Li, H., Li, F., Fan, C.H., Zhang, H., 2013a. J. Am. Chem. Soc. 135, 5998-6001.
768 Zhu, W.P., Zhao, Z.W., Li, Z., Li, H., Jiang, J.H., Shen, G.L., Yu, R.Q., 2013b. New J. Chem. 37,
769 927-932.
770 Zhuang, H.L., Zhen, S.J., Wang, J., Huang, C.Z., 2013. Anal. Methods 5, 208-212.
771 Zuo, P., Li, X.J., Dominguez, D.C., Ye, B.C., 2013. Lab Chip 13, 3921-3928.
772

Table 1

Graphene-based transducers for electrochemical aptasensors.

Analyte	Transducer	Signal molecule	Immobilization method for aptamer	Electrochemical technique	Linear range	Detection limit	Ref.
Label							
ATP	MGNs	Fc	Physical adsorption	SWV	1.0×10^{-3} - 300 μM	0.1×10^{-3} pM	(Tang et al., 2011a)
ATP	MGNs	Fc	Physical adsorption	SWV	1.0×10^{-6} - 500 μM	0.1 pM	(Tang et al., 2011b)
Cocaine		Th			1.0×10^{-5} - 400 μM	1.5 pM	
Cocaine	GNs/AuNPs	*p*-APP (AP)	Au-S	DPV	1.0×10^{-3} - 0.5 μM	1.0×10^{-3} pM	(Jiang et al., 2012a)
L-histidine	GNs-AuNPs	Fc	Au-S	SWV	1.0×10^{-5} - 10 μM	0.1 pM	(Liang et al., 2011)
HL-60 cell	GNs-AuNPs	Aq	Au-S	DPV	5×10^{2} - 1×10^{7} cells/mL	350 cells/mL	(Zheng et al., 2013)
CEM cell		Th					
Thrombin	GNs-PTCDA/AuNPs	H_2O_2 (HRP)	Au-S	CA	1.0×10^{-6} - 1.0 nM	0.65×10^{-3} pM	(Peng et al., 2012)
Thrombin	GNs-PANI-AuNPs	GOD	Au-S	CV	1.0×10^{-3} - 30 nM	0.56 pM	(Bai et al., 2013)
Thrombin	GNs-SWCNTs/AuNPs/NiHCFNPs/AuNPs	H_2O_2 (HRP)	Au-S	DPV	1.0×10^{-2} - 50 nM	2.0 pM	(Yuan et al., 2011a)
Thrombin	GNs-PAMAM	Th	Amide	DPV	1.0×10^{-4} - 80 nM	0.05 pM	(Zhang et al., 2013a)
PDGF	GNs-PDDA-AuNPs	GOD	Au-amino	CV	5.0×10^{-3} - 60 nM	1.7 pM	(Deng et al., 2013)
PDGF	OGNs/AuNPs	AA-P (AP)	Au-amino	DPV	2.0×10^{-3} - 40 nM	0.6 pM	(Han et al., 2013)
Label free							
Thrombin	GQDs	$[Fe(CN)_6]^{3-/4-}$	Physical adsorption	DPV	200 - 500 nM	0.1 pM	(Zhao et al., 2011)
Thrombin	GNs-NA/MB/AuNPs	MB	Au-S	DPV	0.01 - 50 nM	6.0 pM	(Sun et al., 2011a)
Thrombin	GNs-PTCA/AuNPs	PTCA	Au-S	DPV	1.0×10^{-3} - 40 nM	0.2 pM	(Yuan et al., 2011b)
Thrombin	GNs-NA-NiHCFNPs/AuNPs	$[Fe(CN)_6]^{3-/4-}$	Au-S	CV	1.0×10^{-3} - 1.0 nM	0.3 pM	(Jiang et al., 2012b)
Thrombin	GNs-Tb-AuNPs	Tb	Au-S	CV	1.0×10^{-3} - 80 nM	0.33 pM	(Xie et al., 2012b)
Thrombin	GNs-Th/AuNPs	Th	Au-S	DPV	0.5 - 40 nM	0.093 nM	(Zhang et al., 2013d)
Thrombin	$(GNs\text{-}PAA/CdSeNPs)_5$	AA	Phosphoramidate	PEC	1.0×10^{-3} - 1.0×10^{-2} nM	0.45 pM	(Zhang et al., 2011b)
Thrombin	GNs-CS	$[Fe(CN)_6]^{3-/4-}$	Amide	DPV	1.0×10^{-6} - 1.0×10^{-4} nM	0.45×10^{-3} pM	(Wang et al., 2012e)
Thrombin	GNs-Orange II	Orange II	Physical adsorption	DPV	1.0×10^{-3} - 0.4 nM	0.35 pM	(Guo et al., 2013)
Lysozyme					5.0×10^{-3} - 0.7 nM	1.0 pM	
Lysozyme	GNs-CS	$[Fe(CN)_6]^{3-/4-}$	Amide	EIS	10 - 500 nM	6.0×10^{-3} pM	(Xiao et al., 2013)
Lysozyme	GNs/Fe_2O_3	$[Fe(CN)_6]^{3-/4-}$	Electrostatic adsorption	EIS	5.0 - 5.0×10^{3} ng/mL	0.16 ng/mL	(Du et al., 2013a)
D-VP	GNs-Polyelectrolyte-MB	MB	Electrostatic adsorption	DPV	1.0 - 265 ng/mL	1.0 ng/mL	(Qin et al., 2012)
D-VP	GNs-MS-AuNPs/PEI-Fc	Fc	Au-S	DPV	5.0 - 56.5×10^{3} ng/mL	5.0 ng/mL	(Du et al., 2012b)
ATP	GNs-Porphyrin	Porphyrin	Physical adsorption	DPV	2.2×10^{-3} - 1.3 μM	0.7 nM	(Zhang et al., 2012b)
Dopamine	GNs-PANI	$[Fe(CN)_6]^{3-/4-}$	Phosphoramidate	SWV	7.0×10^{-3} - 90 nM	1.98 pM	(Liu et al., 2012a)
HeLa cell	GNs-PTCA	$[Fe(CN)_6]^{3-/4-}$	Amide	EIS	1.0×10^{3} - 1.0×10^{6} cells/mL	794 cells/mL	(Feng et al., 2011)
SK-BR-3 cell	GNs-ZnO/AuNPs	AA	Au-amino	PEC	1.0×10^{2} - 1.0×10^{6} cells/mL	58 cells/mL	(Liu et al., 2014)

ATP: adenosine triphosphate; MGNs: magnetic graphene nanosheets; Fc: ferrocene; SWV: square wave voltammetry; Th: thionine; GNs: graphene nanosheets; AuNPs: gold nanoparticles; SWCNTs: single-walled carbon nanotubes; NiHCFNPs: nickel hexacyanoferrate nanoparticles; HRP: horseradish peroxidases; DPV: differential pulse voltammetry; *p*-APP: *p*-amino phenyl phosphate; AP: alkaline phosphatase; PTCDA: 3,4,9,10-perylene tetracarboxylic dianhydride; CA: chronoamperometry; PANI: polyaniline; GOD: glucose oxidase; CV: cyclic voltammetry; Aq: anthraquinone; PDGF: platelet-derived growth factor; PDDA: poly(diallyldimethylammonium chloride); OGNs: onion-like mesoporous graphene nanosheets; AA-P: ascorbic acid 2-phosphate; PAMAM: carboxyl-terminated polyamidoamine; GQDs: graphene quantum dots; D-VP: D-vasopressin; MB: methylene blue; EIS: electrochemical impedance spectroscopy; NA: Nafion; PTCA: 3,4,9,10-perylene tetracarboxylic acid; Tb: toluidine blue; MS: mesoporous silica; PEI: poly(ethyleneimine); CS: chitosan; PAA: poly(acrylic acid); AA: ascorbic acid; PEC: photoelectrochemistry.

Table 2

Graphene and its derivatives-based nanocarriers for electrochemical aptasensors.

Analyte	Nanocarrier	Signal molecule	Electrochemical technique	Linear range	Detection limit	Ref.
Graphene						
Thrombin	GNs-HCoPt-Th-HRP-TBA	H_2O_2	DPV	1.0×10^{-3} - 50 nM	0.34 pM	(Wang et al., 2011c)
Thrombin	GNs-PAMMA-Th-TBA-hemin-BSA	NADH	DPV	2.0×10^{-4} - 30 nM	0.1 pM	(Yuan et al., 2013)
Thrombin	GNs-PdNPs-Tb-TBA-hemin-BSA	NADH	DPV	1.0×10^{-4} - 50 nM	0.03 pM	(Xie et al., 2012a)
Thrombin	GNs-PDDA-PtNPs/TBA-GOD	Glucose	DPV	3.0×10^{-4} - 35 nM	0.21 pM	(Bai et al., 2012a)
Thrombin	GNs-Fc-PtNPs-TBA/GOD-HRP	Fc	DPV	0.02 - 45 nM	11.0 pM	(Bai et al., 2012b)
PDGF	GNs-Tb-PtNPs-PBA/GOD-HRP	Tb		0.01 - 35 nM	8.0 pM	
IgE	GNs-AgNPs-Ab	AgNPs	SWASV	1.0×10^{-2} - 1.0 μg/mL	3.6 ng/mL	(Song et al., 2013)
Graphene oxide						
Thrombin	GONs-$(AP\text{-}AuNPs)_2$-TBA	AA-P	DPV	8.0×10^{-3} - 15 nM	2.7×10^{-3} pM	(Wang et al., 2012d)
Thrombin	GONs-TBA	H_2O_2	DPV	5.0×10^{-4} - 20 nM	0.15 pM	(Xu et al., 2013b)
Thrombin	GONs-MB	MB	DPV	0.028 - 3.7 nM	3.05 pM	(Chen et al., 2013)
ATP				0.1 - 500 nM	29.1 pM	

GNs: graphene nanosheets; HCoPt: hollow CoPt bimetal alloy nanoparticles; Th: thionine; HRP: horseradish peroxidases; TBA: thrombin binding aptamer; DPV: differential pulse voltammetry; PAMMA: carboxyl-terminatedpolyamidoamine; BSA: bovine serum albumin; NADH: nicotinamide adenine dinucleotide; PdNPs: palladium nanoparticles; Tb: toluidine blue; PDDA: poly(diallyldimethylammonium chloride); PtNPs: platinum nanoparticles; GOD: glucose oxidase; IgE: immunoglobulin E; AgNPs: silver nanoparticles; Ab: antibody; SWASV: square wave anodic stripping voltammetry; PDGF: platelet-derived growth factor; PBA: PDGF binding aptamer; Fc: ferrocene; GONs: graphene oxide nanosheets; AP: alkaline phosphatase; AuNPs: gold nanoparticles; AA-P: ascorbic acid 2-phosphate; ATP: adenosine triphosphate; MB: methylene blue.

795 **Table 3**

796 Graphene oxide as an effective fluorescence nanoquencher in fluorescent aptasensors.

Analyte	Fluorescent reporter	Linear range	Detection limit	Sample	Comments	Ref.
Normal						
ATP	FAM	10 - 2.5×10^3 μM	-	JB6 cells	First example of using GO-based fluorescent assay for molecule probing in living cells	(Wang et al., 2010b)
ATP	FAM	5.0 - 2500 μM	2.0 μM	Cancer cell	Long range resonance energy transfer	(He et al., 2011)
ATP	FAM	3 - 320 μM	0.45 μM	-	'Turn off' detection mode and a fluorescein-labeled complementary DNA was used as signal reporter	(Pu et al., 2012)
Ochratoxin A	FAM	50 - 500 nM	21.8 nM	Red wine	Poly(vinyl pyrrolidone) coated GO nanosheets to repel physical adsorption of ochratoxin A	(Sheng et al., 2011)
Ochratoxin A Fumonisin B_1	UCNPs-Er UCNPs-Tm	0.05 - 100 ng/mL 0.1 - 500 ng/mL	0.02 ng/mL 0.1 ng/mL	Maize	Multiplexed analysis	(Wu et al., 2012)
Mucin 1	Cy5	0.04 - 10 μM	28 nM	Serum	'Turn on' detection mode with low background fluorescence	(He et al., 2012b)
PDGF	FAM	0.167 - 1.167 nM	167 pM	Serum	'Turn on' detection mode and high specificity	(Liang et al., 2013)
VEGF	FAM	0.5 - 5.0 nM	0.25 nM	Serum	'Turn on' detection mode and lower detection limit compared to other optical assays	(Wang and Si, 2013)
ADA	FAM	1.54 - 28.6 nM	1.54 nM	Serum	Competitive assay	(Xing et al., 2012)
Zeatin	FAM	3.0 - 50 μM	0.1 μM		No response to the analogs of zeatin	(Qi et al., 2013)
K^+	Ru^+	50 - 500 μM	-	-	Label-free and K^+ stabled G-rich ssDNA as aptamer	(Sun et al., 2011b)
S. aureus S. enterica	Cy3	10^4 - 10^6 cfu/mL 42.2 - 675 cfu/mL	800 cfu/mL 61 cfu/mL		Multiplexed analysis using microfluidic biochip	(Zuo et al., 2013)
Coralyne	TAMRA	10 - 700 nM	-	Urine	Long range resonance energy transfer and cell imaging	(Zhang et al., 2013c)
PrP	TAMRA	10.2 - 78.8 μg/mL	0.309 μg/mL		Long range resonance energy transfer	(Zhuang et al., 2013)
Amplification						
Theophylline TPP	FAM	0.1 - 10 μM 0.5 - 100 μM	0.1 μM 0.5 μM		DNase I and aptazyme	(Li et al., 2013c)
Insulin	FAM	-	5.0 nM		DNase I	(Pu et al., 2011)
ATP	FAM	0.1 - 1.0×10^3 μM	40 nM		DNase I	(Lu et al., 2010)
ATP	FAM	5.0×10^{-3} - 100 μM	1.0 nM		Exo III	(Hu et al., 2012)
ATP	SYBR Green I	1.0×10^{-3} - 0.2 μM	0.2 nM		Exo III and Label-free	(Zhu et al., 2013b)
Lysozyme	FAM	0.125 - 1 μg/mL	0.08 μg/mL		Exo III	(Chen et al., 2012a)
IFN-γ	FAM	3.5×10^{-3} - 1.0 pM	1.5 fM	Plasma	KF Polymerase	(Hu et al., 2013)
Cocaine	SYBR Green I	0.2 - 100 μM	190 nM	Urine	KF Polymerase and Label-free	(Qiu et al., 2013)

797 ATP: adenosine triphosphate; FAM: carboxyfluorescein; Cy5: cyanine-5; PDGF: platelet derived growth factor; VEGF: vascular

798 endothelial growth factor; ADA: Adenosine deaminase; Ru^+: Ru polypyridine complex; UCNPs: upconversion fluorescent

799 nanoparticles; S. aureus: Staphylococcus aureus; S. enterica: Salmonella enterica; Cy3: cyanine-3; PrP: cellular prion protein;

800 DNase I: deoxyribonuclease I; TPP: thiamine pyrophosphate; Exo III: exonuclease III; IFN-γ: interferon-gamma; KF polymerase:

801 Klenow fragment polymerase.

Fig. 1. Schematic illustration of graphene-like two-dimensional nanomaterials-based aptasensors.

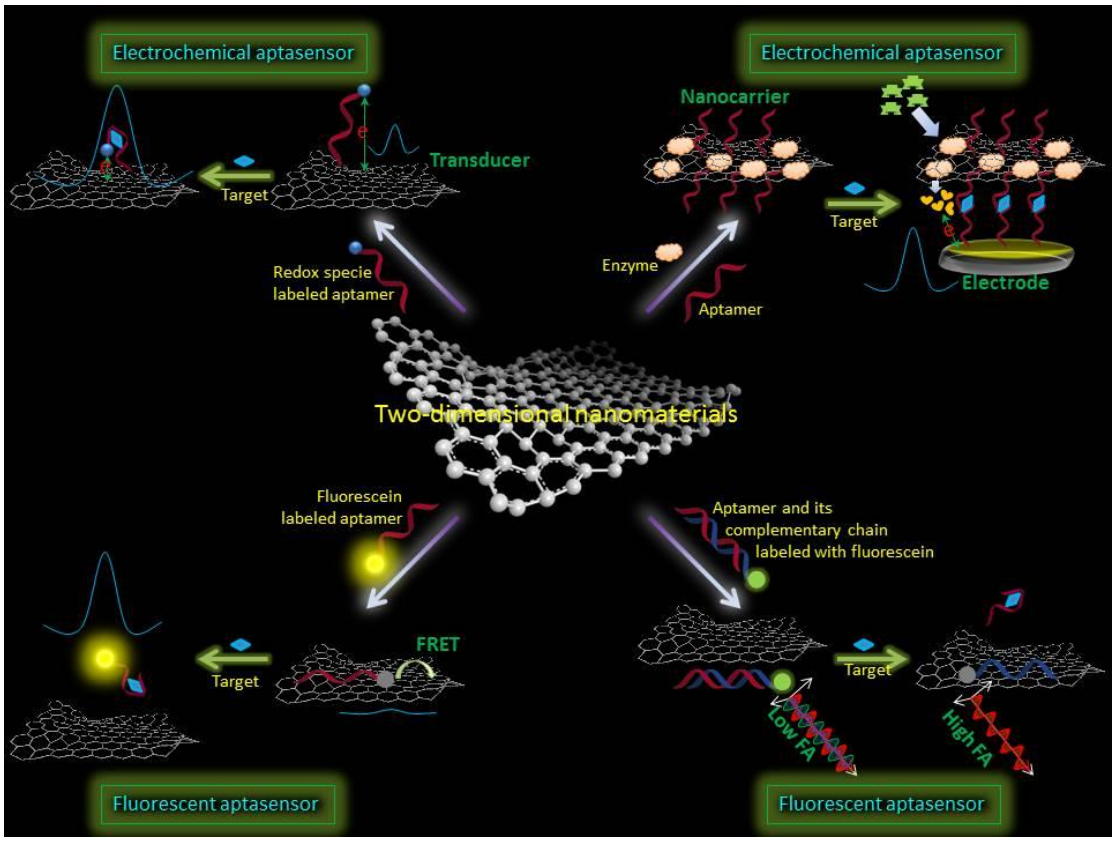

Fig. 2. a) Schematic illustration of the sandwich electrochemical aptasensors for simultaneous detection of HL-60 and CEM cells based on a graphene/AuNPs platform. Reprinted with permission of The Royal Society of Chemistry from reference Zheng et al. (2013). b) Schematic illustration of the multiplexed electrochemical aptasensing assay based on magnetic graphene platform and DNase-I induced signal amplification. Reprinted with permission of American Chemical Society from reference Tang et al. (2011b).

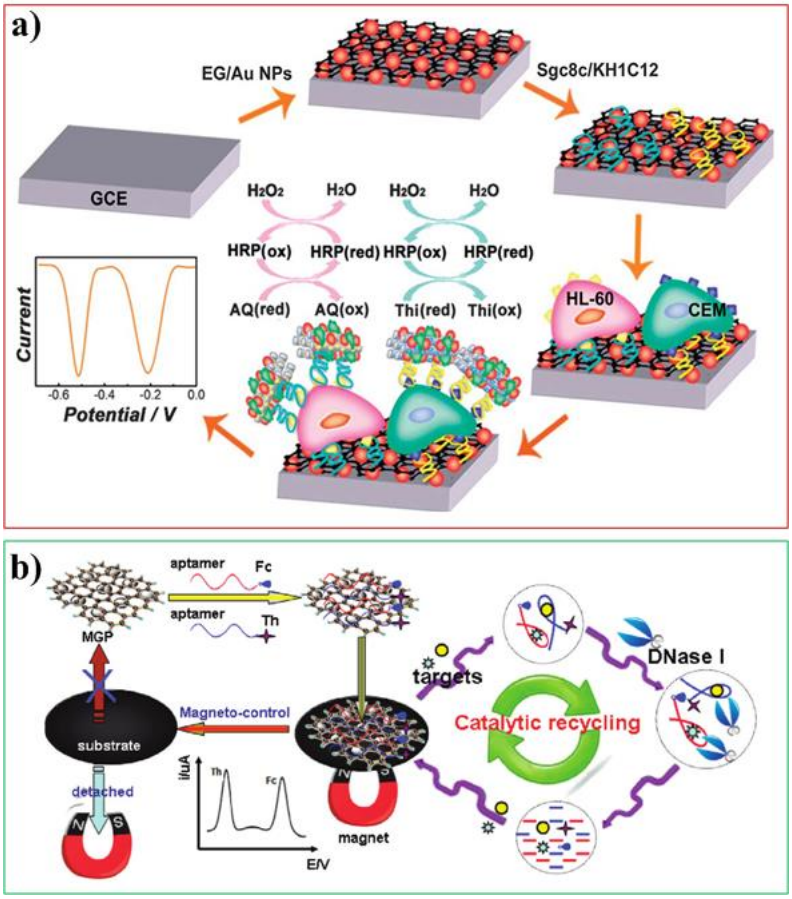

Fig. 3. a) Fabrication steps for the different graphene-based nanocarriers and the sandwich aptasensor. Reprinted with permission of Elsevier from reference Bai et al. (2012b). b) Illustration of the utilization of GONPs as inherently electroactive labels for thrombin detection. (A) In the presence of THR, the aptamer bound specifically to thrombin and resulted in partial removal of immobilized aptamer from the electrode surface due to conformational changes. GONPs then adsorbed onto the remaining immobilized aptamer due to the strong π-π interactions. (B) In the absence of thrombin, GONPs were adsorbed onto the immobilized aptamer. Reprinted with permission of The Royal Society of Chemistry from reference Loo et al. (2013b).

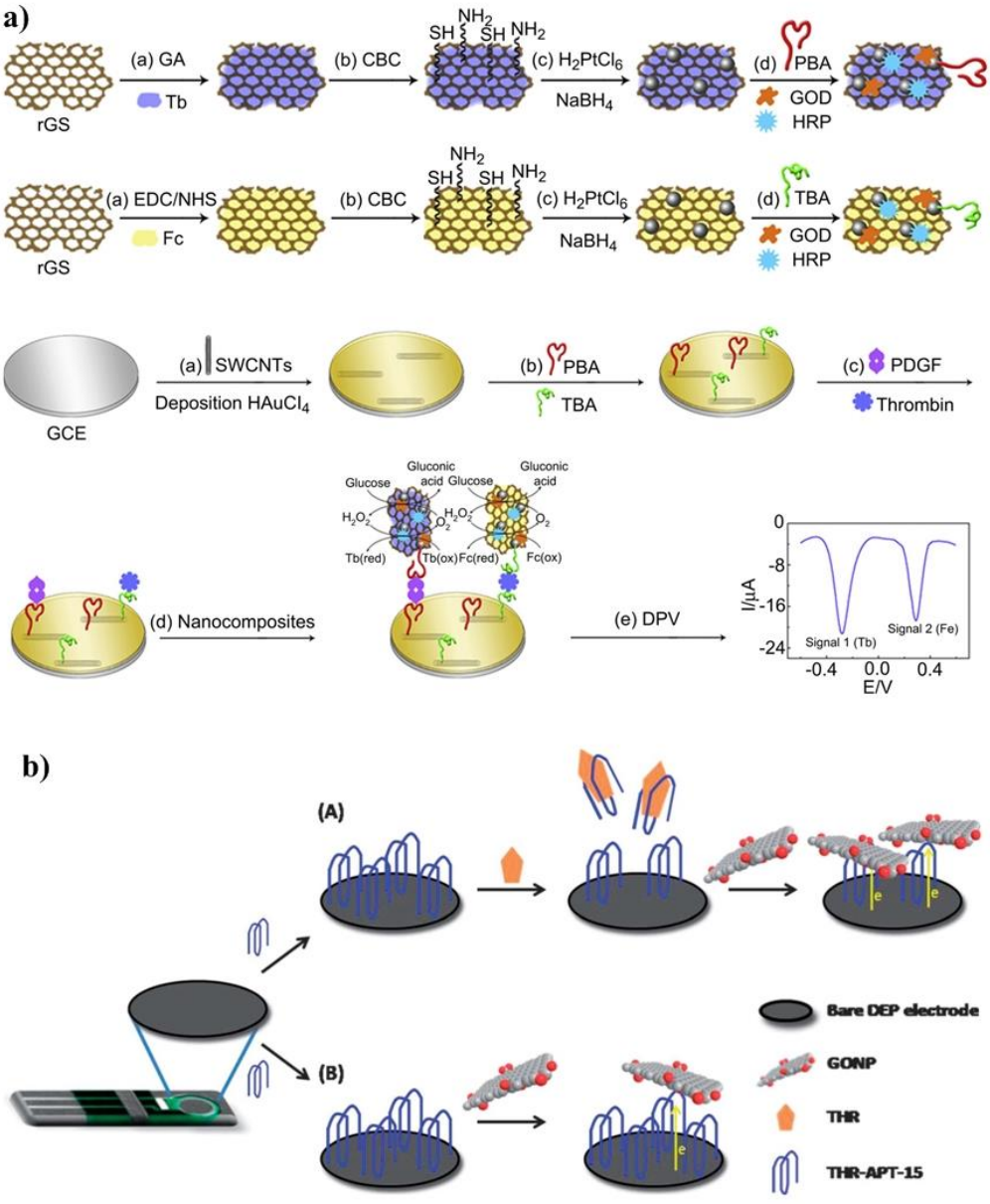

Fig. 4. Illustration of the (a) classic mode, (b) amplified mode-DNase I, and (c) amplified mode-polymerase in the GO-based FRET aptasensors. Reprinted with permissions of John Wiley & Sons from reference Lu et al. (2010) and Elsevier from reference Hu et al. (2013).

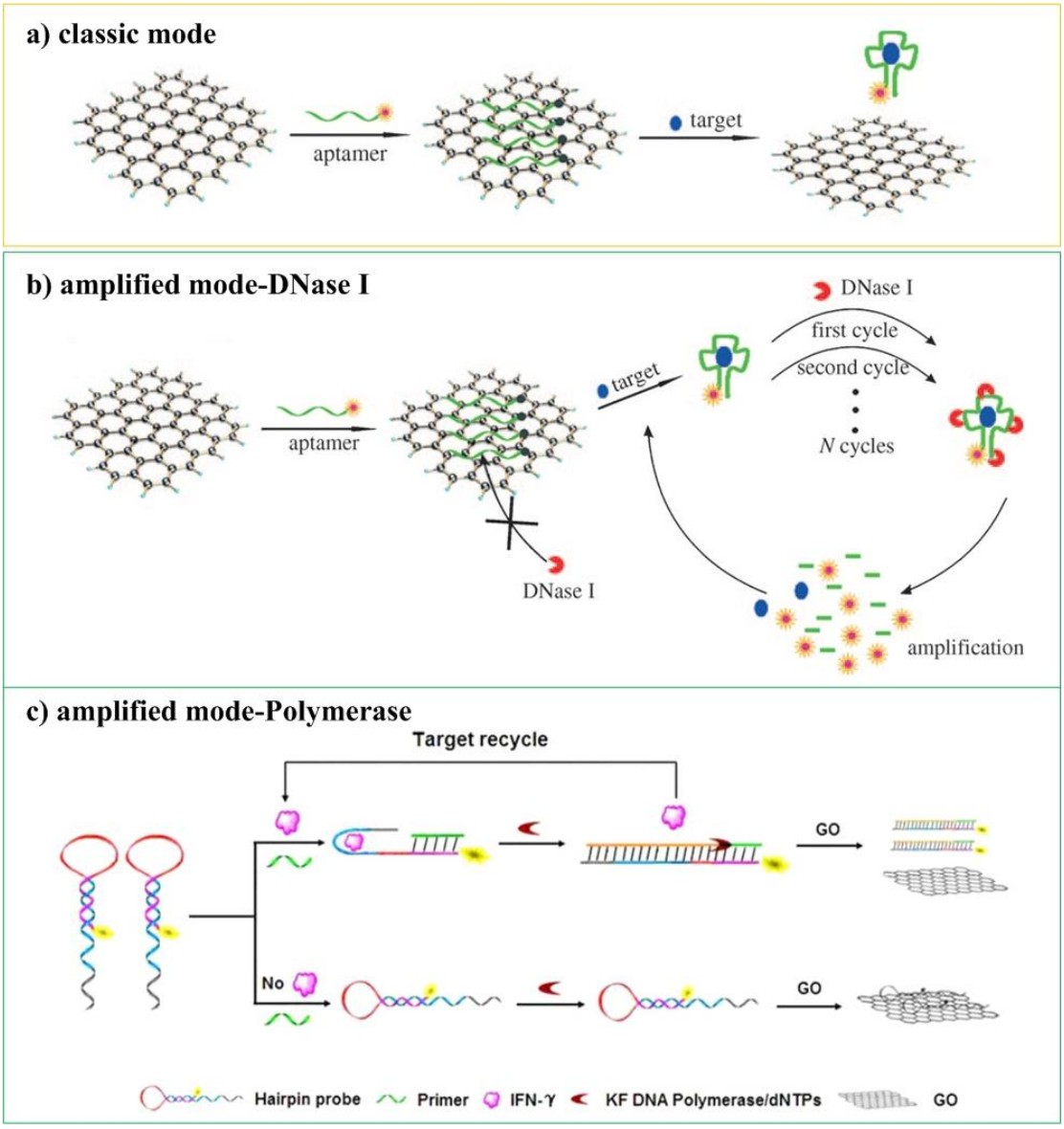

Fig. 5. Schematic representation of (a) the LbL-assembled GO multilayer array and (b) the aptamer-based protein sensing mechanism of the GO multilayer array. (c) multiplex detection of four different proteins using their FAM-labeled binding aptamers and (d) selective fluorescence recovery of the PDGF aptamer-coated GO spot upon PDGF addition. Plus and minus sign respectively indicate the loading and unloading of both specific FAM-labeled aptamers and proteins onto the positions. Reprinted with permission of Nature Publishing Group from reference Jung et al. (2013).

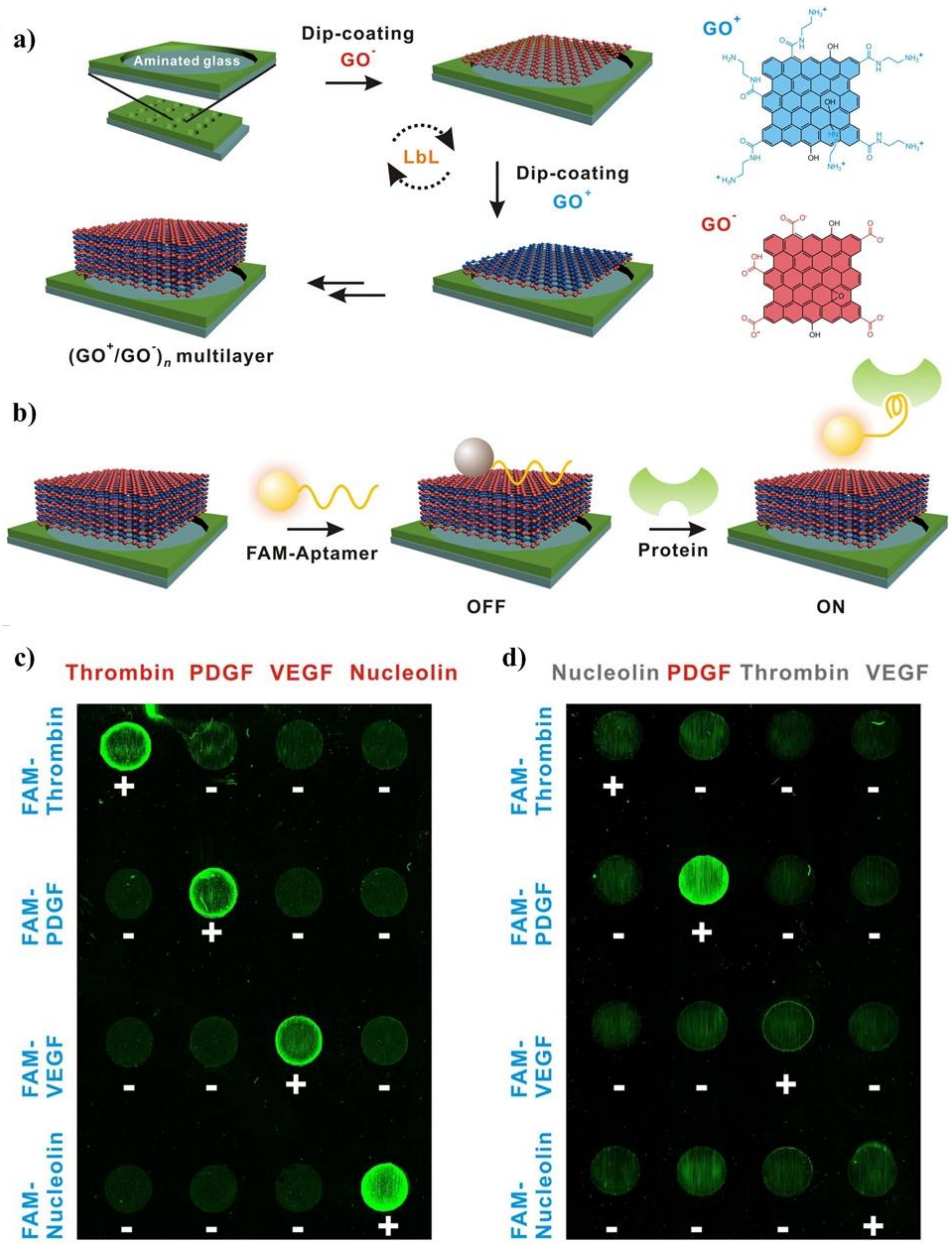

Fig. 6. Schematic illustration of (a) MoS_2 nanosheets- and (b) MnO_2 nanosheets-based FRET aptasensors. Reprinted with permissions of The Royal Society of Chemistry from references Ge et al. (2014) and Yuan et al. (2014).

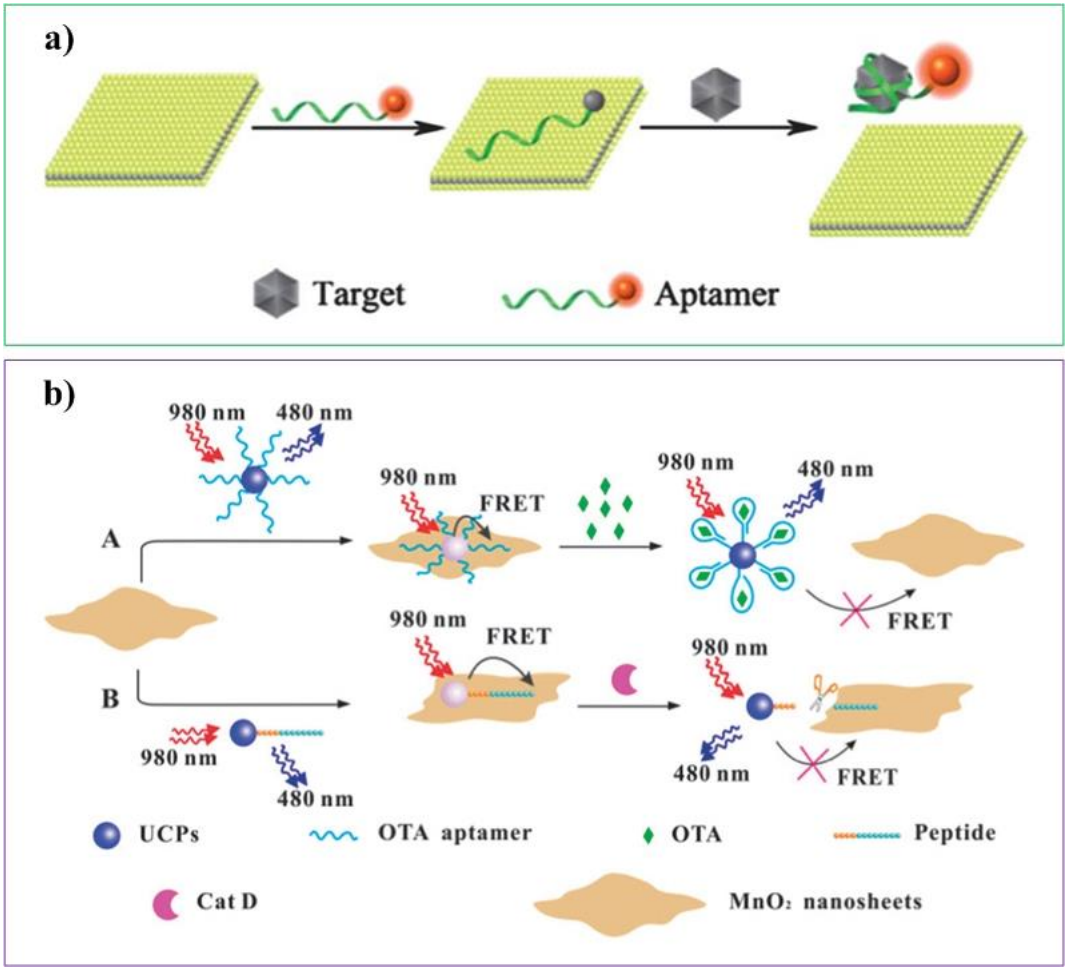

Fig. 7. General strategies for GO-based signal amplification assay of small molecule target with (a) FA reduction and (b) FA enhancement detection. Reprinted with permission of American Chemical Society from reference Liu et al. (2013b).

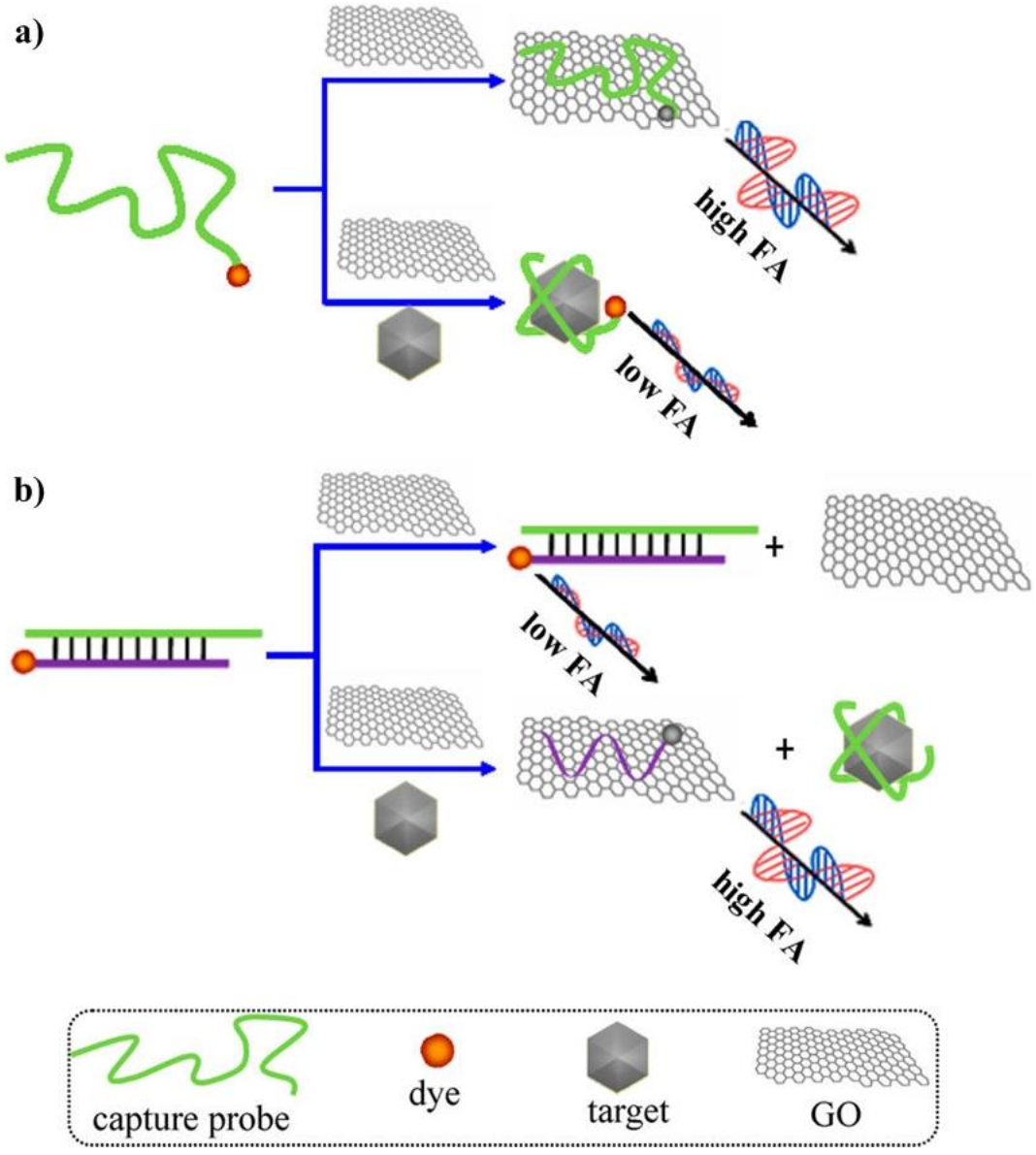

Fig. 8. (a) FET based on polypyrrole-converted nitrogen-doped few-layer graphene as channel; (b) Schematic illustration of the use of AuNPs to construct sandwich aptasensor based on graphene-based FET; (c) Fabrication steps of graphene-based SPR aptasensor. Reprinted with permissions of American Chemical Society from reference Kwon et al. (2012), John Wiley & Sons from reference Kim et al. (2013), and The Royal Society of Chemistry from reference Wang et al. (2011a).